Supplementary Information

Cellulose-based hybrid 2D material aerogel for flexible all-solid-state supercapacitor with high specific capacitance

Yanyan Lv,[a] Lei Li,[a] Yi Zhou,[a] Miao Yu,[a] Jianquan Wang,[a] Jianxin Liu,[a] Jiagui Zhou,[b]Zongqing Fan[b] and Ziqiang Shao*[a]

[a] *Beijing Engineering Research Centre of Cellulose and Its Derivatives, School of Materials Science and Engineering, Beijing Institute of Technology, Beijing 100081, P. R. China.*

[b]*Hubei Jinhanjiang Refined Cotton Co. Hubei 431900, P. R. China.*

**E-mail: shaoziqiang@263.net*

Preparation of CNFs suspension

CNFs were prepared according to the literature methodology reported by Isogai, [S1] and described in brief as follows: TEMPO (0.0495 g) and NaBr (0.495 g) were dissolved in deionized water (400 mL) with continuous stirring. Next, hardwood bleached kraft pulps (3 g) were added after the catalysts have been completely dissolved. The oxidation reaction was started by adding the desired amount of the NaClO solution (15 mmol g^{-1} cellulose). Then 0.5 M NaOH was added to maintain the pH of the reaction solution at about 10.00-10.50 at 10℃until the pH remained essentially constant that indicated the oxidation reaction ended. And then the TEMPO-oxidized cellulose was washed thoroughly with deionized water by filtration for at least 3 times. After that, 2 mg mL^{-1} oxidized cellulose/water slurries were sonicated for 20 min at power of 300 W in an ice bath. Following, transparent CNFs dispersion was prepared by centrifuging at 9800 rpm for 20 min to remove the unfibrilated cellulose. The last the transparent CNFs dispersion was stored at 4℃ before use.

Preparation of MoS_2 powder

The MoS_2 were synthesized via a hydrothermal route and described in brief as follows: 0.24 g $Na_2MoO_4{\cdot}2H_2O$ was dissolved in 40 mL deionized water. Then 0.60 g L-cysteine was added after the Na_2MoO_4 has been completely dissolved and the

mixture was diluted with deionized water to 70 mL, and then the solution was violently stirred for about 1 h. Subsequently, the mixture was transferred into a 100 mL Teflon-lined stainless steel autoclave and heated at 200℃ for 24 h. After cooling naturally, the black MoS_2 composites were collected by filtration, washed with distilled water and absolute ethanol for several times, and then dried in vacuum at 60℃ for 24 h.

Preparation of GO suspension

The synthesis of dispersions of GO were produced using a modified Hummers' method[S2] from graphite powder and described in brief as follows: Graphite powder (5 g) was added into 100 ml beaker containing concentrated H_2SO_4 (25 ml), $K_2S_2O_8$ (5 g), P_2O_5 (5 g) with continuous stirring at 80 ℃. The resulting mixture was kept at 80 ℃ for 4.5 h in oil bath, then DI water (~1 L) was added to the resulting mixture and left overnight. Pretreated graphite was thoroughly washed with water by filtration to remove all soluble substances and then dried in the oven at 60 ℃. Pretreated graphite was added into 1000 ml beaker containing concentrated H_2SO_4 (230 ml) in ice bath. $KMnO_4$ (30 g) was added slowly to dissolve completely. The resulting mixture was allowed to react at 35 ℃ for hours, and then 460 ml DI water was slowly added. In the process of adding water, the temperature of the mixture was remained constant. Another 1.4 L DI water was added to the mixed solution with continuous stirring at room temperature for 2 h. Afterward, 25 ml of 30% H_2O_2 was added to the mixture with continuous stirring at room temperature. The color of the mixed solution becomes golden yellow. The resulting mixture was stand for about 12h and then the supernatant was decanted. The graphite oxide was thoroughly washed with 5% HCl solution and then DI water to remove all soluble substances. 8 $mg \cdot ml^{-1}$ graphite oxide was sonicated for 20 min using an ultrasonic generator at an output powder of 800 W. The graphene oxide solution was centrifuged at 9800 r/m for 5 min to remove the

unexfoliated graphite oxide. The inorganic ions in graphene oxide suspension were removed by dialysis.

Electrochemical characterization

The electrochemical performances of all-solid-state flexible supercapacitors were tested by cyclic voltammetry (CV), galvanostatic charge/discharge (GCD), and electrochemical impedance spectroscopy (EIS, on a CHI 660D, CH Instruments, Inc). All the electrochemical parameters are calculated as follows,

The gravimetric capacitance:

$C_g=4(\int idV)/(v\times m\times V)$ (CV curves) or $C_g=4I\times\Delta t/(\Delta V\times m)$ (GCD curves)

The area capacitance:

$$C_s=(\int idV)/(v\times S\times V)$$

The specific capacitance of supercapacitor devices:

$$C_{sp}= I\times\Delta t/(\Delta V\times m)$$

$$E=(1/2)\ C_{sp}\times V_{IR}^2$$

$$P= V_{IR}^2/(4m\times R_{ESR})$$

Where I is the applied current, Δt is the discharged time, ΔV is the discharged potential, m is the total mass of two symmetrical electrodes (based on the total mass of MoS_2 and RGO), V_{IR} is voltage after IR drop, v is the voltage scan rate, V is the cell voltage, and S is the area of the supercapacitor.

For the supercapacitor, the area made accessible to the electrolyte was 2.0 cm^{-2}, corresponding to a mass of 2.0 mg of the active materials (MoS_2 and RGO) per electrode. The areal density of the active materials was calculated to be 1mg cm^{-2} per electrode.

Photograph

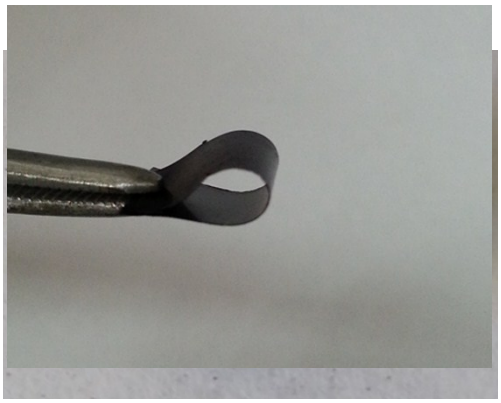

Fig. S2 Demonstration of the flexibility of CNFs/MoS_2/RGO nanohybrid aerogel film

Fig. S1 Photograph of the CNFs/MoS_2/RGO nanohybrid aerogel

Fig. S3 Photograph of the CNFs/MoS_2/RGO all-solid-state flexible supercapacitor

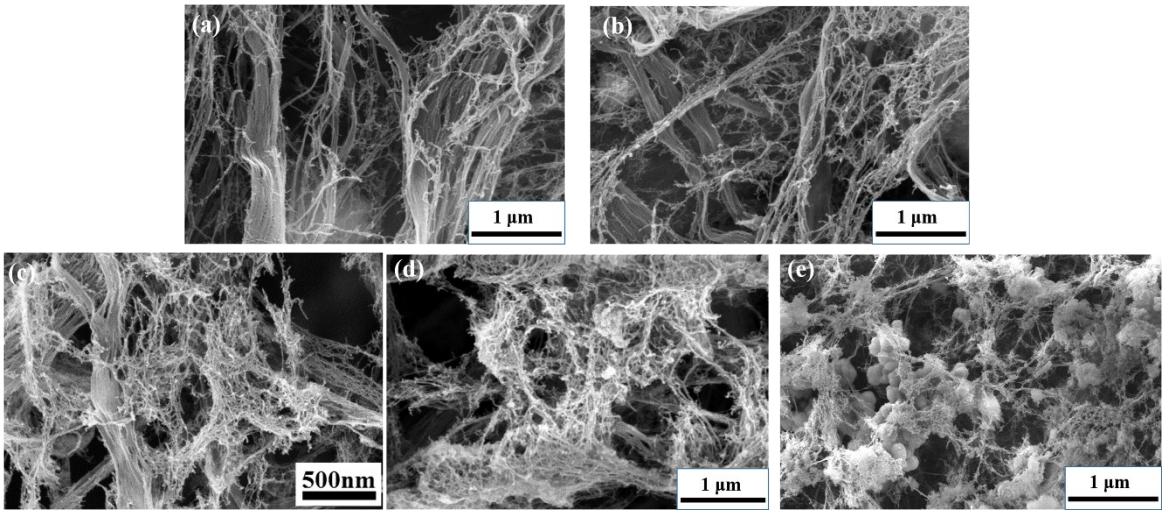

Fig. S4 SEM images of different weight percentages of MoS_2 in the CNFs/MoS_2 aerogels, (a) 10%, (b) 20%, (c) 30%, (d) 40%, (e) 50%.

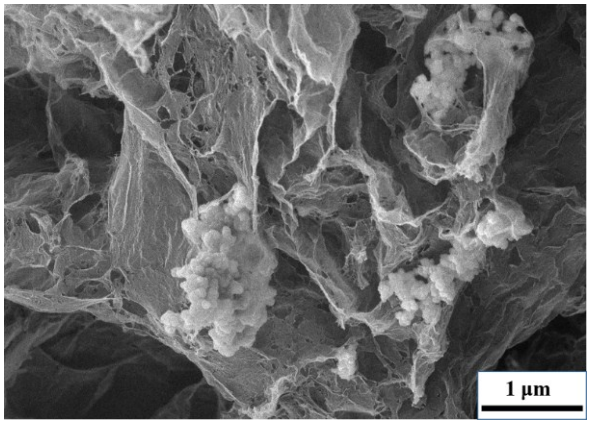

Fig. S5 SEM image of MoS_2/RGO hybrid aerogel without CNFs

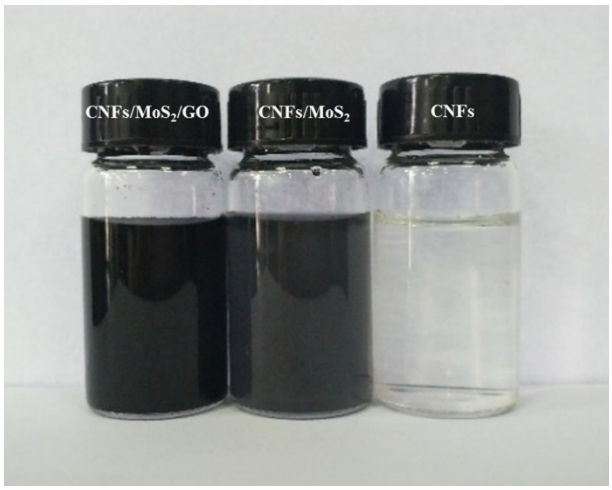

Fig. S6 Optical images of the aqueous dispersion of CNFs/MoS_2/GO, CNFs/MoS_2 and CNFs suspension.

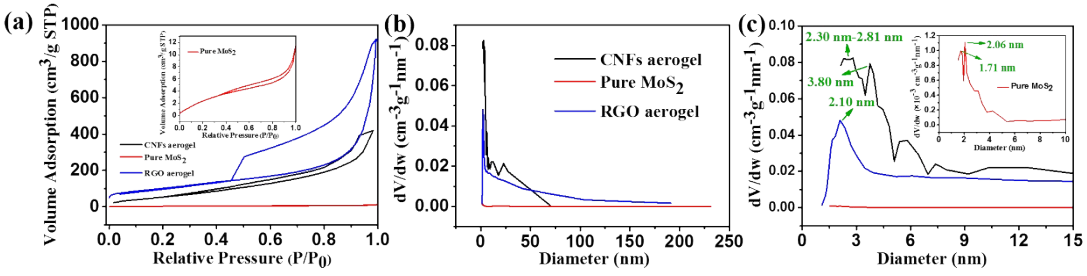

Fig. S7 (a) N_2 adsorption/desorption isotherms of CNFs aerogel, pure MoS_2, RGO aerogel. The inset is an enlarged view of the N_2 adsorption/desorption isotherm of MoS_2. (b) BJH pore size distribution curves of CNFs aerogel, pure MoS_2, RGO aerogel. (c) The enlarged view of (b). The inset is an enlarged view of the BJH pore size distribution curve of MoS_2.

Table S1. The specific electrode capacitance of some graphene and MoS_2-based supercapacitors

Materials	Specific capacitance (F g^{-1})	Source
CNFs/MoS_2/RGO aerogel film	916.42	Our work
CNF/RGO/MoOxNy aerogel film	680	J. Mater. Chem. A, 2017[S3]
CNFs/RGO/CNT aerogel film	252	ACS Appl. Mater. Interfaces, 2015[S4]
MoS_2/RGO	265	Adv. Energy Mater., 2014[S5]
PANI/MoS_2	575	Electrochimica Acta., 2013[S6]
MoS_2	114	J. Nanosci. Nanotechnol.,2014[S7]
CNFs/RGO aerogel film	207	J. Mater. Chem. A, 2013[S8]
RGO aerogel film	172	Adv. Mater., 2012[S9]
Solvated graphene film	215	Adv. Mater., 2011[S10]
GO	189	Energy Environ. Sci., 2011[S11]
CNPs/RGO	198	Energy Environ. Sci., 2011[S12]
RGO/cellulose	120	Adv. Energy Mater., 2011[S13]
RGO aerogel	128	J. Mater. Chem, 2011[S14]

Table S2. The capacitance per geometric area of some flexible or thin-film supercapacitors

Materials	Areal capacitance (mF cm^{-2})	Source
CNFs/MoS_2/RGO aerogel film	458	Our work
CNFs/RGO/CNT aerogel film	216	ACS Appl. Mater. Interfaces, 2015[S4]
CNFs/RGO aerogel film	158	J. Mater. Chem. A., 2013[S8]
Porous RGO film	45.6	Adv. Mater., 2012[S15]
CNTs/bacterial cellulose paper	18.8	ACS Nano., 2012[S16]
Graphene/cellulose paper	81	Adv. Energy. Mater., 2011[S13]
SWCNT/cotton paper	34	Nano Res.,2010[S17]
CNT coating on paper	160	PNAS., 2009[S18]

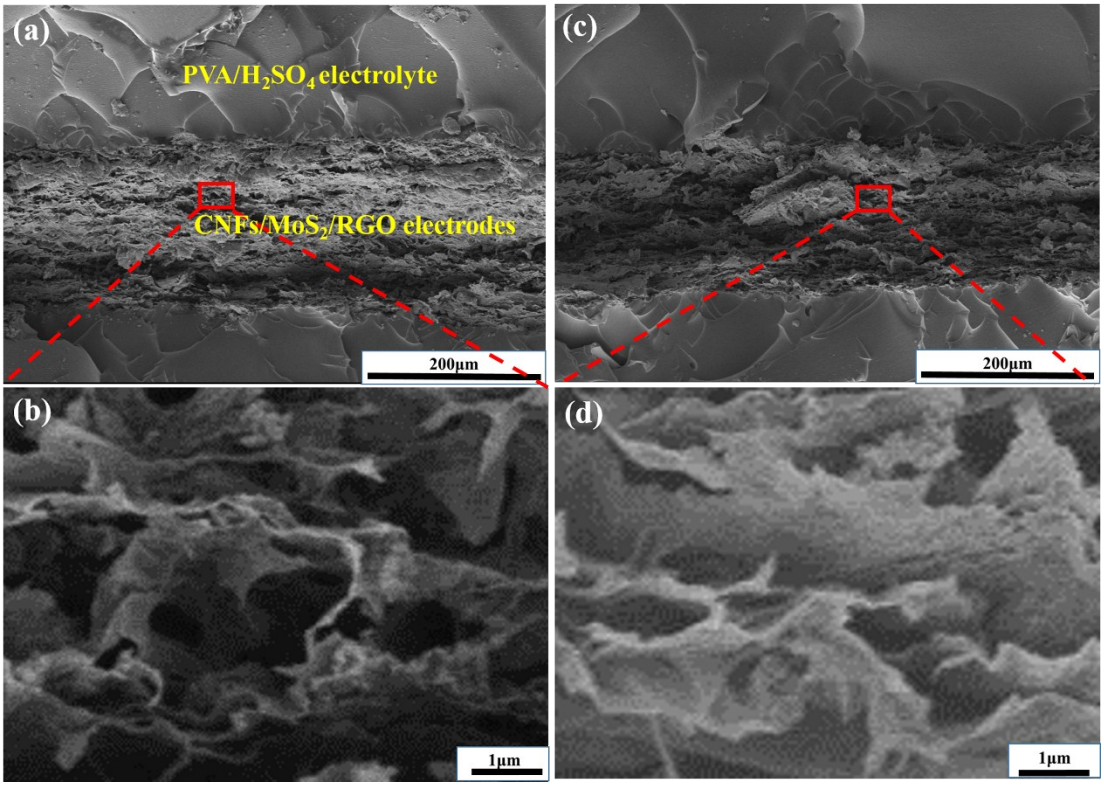

Fig. S8 SEM image of the cross-section of the CNFs/MoS_2/RGO aerogel electrode infiltrated with H_2SO_4/PVA gel electrolyte: (a) before cyclic test, (b) the enlarged view of the red area of (a), (c) after 5000 cyclic test, (d) the enlarged view of the red area of (c).

References

S1. A. Isogai, T. Saito and H. Fukuzumi, *Nanoscale*, 2011, **3**, 71-85.

S2. V. C. Tung, M. J. Allen, Y. Yang and R. B. Kaner, *Nat. Nanotechnol.*, 2009, **4**, 25-29.

S3. Q. Zheng, A. Kvit, Z. Cai, Z. Ma and S. Gong, *J. Mater. Chem. A*, 2017, 5, 12528-12541.

S4. Q. Zheng, Z. Cai, Z. Ma and S. Gong, *ACS Appl Mater Interfaces*, 2015, **7**, 3263-3271.

S5. E. G. d. S. Firmiano, *Adv. Energy Mater.*, 2014, **4**, 1301380.

S6. K.-J. Huang, L. Wang, Y.-J. Liu, H.-B. Wang, Y.-M. Liu and L.-L. Wang, *Electrochim. Acta*, 2013, **109**, 587-594.

S7. X. Zhou, B. Xu, Z. Lin, D. Shu and L. Ma, *J. Nanosci. Nanotechno.* 2014, **14**, 7250-7254.

S8. K. Gao, Z. Shao, J. Li, X. Wang, X. Peng, W. Wang and F. Wang, *J. Mater. Chem. A*, 2013, **1**, 63-67.

S9. F. Liu, S. Song, D. Xue and H. Zhang, *Adv. Mater.*, 2012, **24**, 1089-1094.

S10. X. Yang, J. Zhu, L. Qiu and D. Li, *Adv. Mater.*, 2011, **23**, 2833-2838.

S11. B. Xu, S. Yue, Z. Sui, X. Zhang, S. Hou, G. Cao and Y. Yang, *Energy Environ. Sci.*, 2011, **4**, 2826-2830.

S12. C. X. Guo and C. M. Li, *Energy Environ. Sci.*, 2011, **4**, 4504-4507.

S13. Z. Weng, Y. Su, D. W. Wang, F. Li, J. Du and H. M. Cheng, *Adv. Energy Mater*. 2011, **1**, 917-922.

S14. X. Zhang, Z. Sui, B. Xu, S. Yue, Y. Luo, W. Zhan and B. Liu, *J. Mater. Chem.*, 2011, **21**, 6494-6497.

S15. J. Chen, K. Sheng, P. Luo, C. Li and G. Shi, *Adv. Mater.*, 2012, **24**, 4569-4573.

S16. Y. J. Kang, S.-J. Chun, S.-S. Lee, B.-Y. Kim, J. H. Kim, H. Chung, S.-Y. Lee and W. Kim, *ACS nano*, 2012, **6**, 6400-6406.

S17. M. Pasta, F. La Mantia, L. Hu, H. D. Deshazer and Y. Cui, *Nano Res.*, 2010, **3**, 452-458.

S18. L. Hu, J. W. Choi, Y. Yang, S. Jeong, F. La Mantia, L.-F. Cui and Y. Cui, *P. Natl Aca. Sci. USA*, 2009, **106**, 21490-21494.